



Transactions of the 13th International Conference on Structural Mechanics in Reactor Technology (SMiRT 13), Escola de Engenharia - Universidade Federal do Rio Grande do Sul, Porto Alegre, Brazil, August 13-18, 1995

## Development of CFD method to evaluate 3-D flow characteristics for PWR fuel assembly

Imaizumi, M.<sup>1</sup>, Ichioka, T.<sup>2</sup>, Hoshi, M.<sup>3</sup>, Teshima, H.<sup>1</sup>, Kobayashi, H.<sup>4</sup>, Yokoyama, T.<sup>1</sup>

1) Mitsubishi Heavy Ind. Ltd., Kobe Shipyard & Machinery, Kobe, Japan

2) Mitsubishi Heavy Ind. Ltd, Takasago R&D Center, Takasago, Japan

3) Mitsubishi Heavy Ind. Ltd, Yokohama, Japan

4) Nuclear Development Corporation, Ibaragi, Japan

### ABSTRACT

The CFD method to evaluate 3-D flow characteristics for PWR fuel assembly has been developed, in order to improve design approach in the flow dynamics field. The processes of study described here are as follows; (1) The grid spacer for PWR fuel assembly consists of many subchannels called "cell", and they are classified into 4 types hydraulically. First, the analysis model of a typical cell, which is the most representative among the parts, was constructed and calculated.

At the same time, a flow test was conducted using the part of the actual grid spacer (5×5 rod array), and the distribution of the pressure difference around the grid spacer and the pressure drop of the grid spacer were measured to verify this evaluation method. The calculated results show good agreement with the test results, both the distribution of the pressure difference and the pressure drop of the grid spacer, so, this analytical method has been successfully verified.

(2) Next, models for other particular cells such as thimble cell, side cell and corner cell, were also constructed and calculated. The pressure drop of the grid spacer was obtained by composing results of these 4 types of cells. This method has already brought into practical use for design evaluation of the grid spacer.

(3) To investigate the DNB (Departure from Nucleate Boiling) performance, evaluation was carried out, TDC (Thermal Diffusion Coefficient) value and flow intensity of 2 different type grid spacers were compared.

As a result of this study, the correlation between the TDC factor and the flow intensity is confirmed.

From these studies, it was concluded that the evaluation method for the 3-dimensional flow characteristics has been developed and that CFD techniques are quite effective for designing fuel grid spacers.

### 1. INTRODUCTION

There are many essential requests from many design fields in designing the PWR fuel assembly, especially for the fuel grid spacer. For example, the buckling strength in the mechanical design, and the neutron balance in the nuclear design.

From the view point of thermal & hydraulic design, there are 2 main subjects; one is the pressure drop and the other is the DNB performance of the grid spacer, and they have been evaluated by flow test and DNB test with an actual grid spacer. Since usually low pressure drop is preferable and incompatible with the strength of the grid spacer,

designers have to optimize both requests at the same time. One of the solutions to minimize the pressure drop, while keeping certain level of the mechanical strength, is to optimize the mixing vane (M/V) design, such as its size, shape and angle, because this does not contribute to the mechanical strength of the grid spacer, though it produces a rather large pressure drop. But, it used to be difficult to optimize the M/V design that directly influences the DNB performance, because there has been no design approach to optimize that performance. The adequacy of the design could not be confirmed before completing the flow test with an actual grid spacer, since the pressure drop of the grid spacer has been estimated quite roughly according to the calculation handbook, although it forms a complicated shape. Thus, it takes a long time to fix the new design based on this process, because of manufacturing the new type grid spacer for the test.

Nowadays, Computational Fluid Dynamics (CFD) has made remarkable advances and this has made it possible to calculate a flow around a complicated 3-dimensional shaped body. So, we have managed to develop the CFD method to evaluate 3-D flow characteristics for PWR fuel assembly, in order to improve design process in the flow dynamics field.

The 1st subject is to estimate the pressure drop of the grid spacer accurately, the Finite Volume Method (FVM) with the  $k-\epsilon$  turbulence model has been employed for this purpose. A grid spacer for PWR fuel is composed of 4 types of cells, and the analytical model for 'typical cell' which is the most representative among the 4 types of cells, was constructed to analyze the flow around the fuel rods and grid spacer.

To compare the analytical results with the experiment data, a detailed flow test with an actual grid spacer was also conducted.

The analysis which simulated the test was performed, and the calculated distribution of pressure difference was compared with the measured one. They showed fairly good agreement. From the result, it was concluded that this analytical method was verified in predicting the flow characteristics of the grid spacer.

To evaluate the pressure drop of the grid spacer in detail, the analytical models for 3 other types of cells were constructed and analyzed. The pressure drop of the full size grid spacer was obtained from these results.

Through these processes, the flow characteristics of the total grid spacer can be analyzed using the CFD method.

Another approach to evaluate the DNB performance was carried out, by comparing the empirically measured TDC value and calculated flow intensity for 2 different type grids. As a result of this, the correlation between the TDC and the flow intensity was recognized. However, since this study is only one step in approaching the DNB performance evaluation by calculation, further study will be continued.

From these studies, it was concluded that the evaluation method for the 3-dimensional flow characteristics has been developed and that CFD techniques are useful for designing fuel grid spacers.

## 2. Analysis and Experiment for Typical cell

The first subject is to analyze the flow around a grid spacer, in order to estimate the pressure drop. Since a grid spacer for PWR fuel is composed of 4 types of cell, such as typical, thimble, side and corner cell, as shown in Fig. 1. As a first step, the 'typical cell' analysis model was constructed, because of the following 2 reasons;

(1) To verify this analytical method, a flow test was conducted. In the empirical verification, it is necessary to employ the simple model for

both calculation and test, so as to evaluate the accuracy of the method. (2) Since more than half of the flow area of the grid spacer is consist of the typical cells, flow analysis of the cell can be used as the 1st estimation of the pressure drop for a new type grid spacer, when the design change is made.

The finite volume method (FVM) with the  $k-\epsilon$  turbulence model is employed in the analysis. At the same time, a flow test was conducted to verify the analytical method, using a part of the actual grid spacer ( $5 \times 5$  cells size) which is mainly composed of typical cells.

The pressure distribution around the grid spacer was measured, and the analytical results were compared with the test results.

### 2.1 Analysis Model and Analysis Condition

The fuel assembly for PWR bundles using grid spacers. Figs. 2-1 and 2-2 show a fuel assembly and the shape of grid spacer respectively. The analytical model of typical cell shown in Fig. 3, which surrounded by 6 fuel rods. In that figure, the "subchannel" is defined as a flow passage surrounded by 4 fuel rods, so that, the analytical model has 2 sub-channels, because there are 2 types of typical cells, each cell has mixing vanes and they orient at right angle each other (X and Y direction; Fig. 3). For the lateral boundaries of the analytical domain, cyclic boundary condition (B.C) is given, so that the passage surrounded by 6 fuel rods represents a part of an infinitely wide flow field. In the axial direction, the analytical domain covers from 30mm upstream to 180mm downstream from the grid spacer where only one grid spacer exists there. For the axial direction, the calculations were carried out both with or without cyclic B.C. It is obvious that the cyclic B.C simulates the actual one well, since there are several grid spacers for the axial direction in actual condition. On the other hand, it costs 2 or 3 times more to calculate with axial cyclic B.C, than doing it without cyclic B.C; as the final results is obtained after calculating 2 or 3 times. So, to decide the axial B.C, we calculated both cases to evaluate the difference between them. In these calculations, the analytical domain downstream from the grid spacer has been extended up to 400mm, almost the same as the shortest actual grid span length. As a result of these calculations, it is confirmed that as calculated grid loss coefficient there is a difference of about 4% between these results, and since the B.C in the axial direction was decided without cyclic one, this difference is to be considered in the calculated result. The B.C in the axial direction was as follows; the B.C of the upstream side was a uniform flow with a turbulence intensity of 10%, and that of the downstream side was a free outflow. 2 cases of calculations were carried out with different fuel types,  $17 \times 17$  and  $14 \times 14$ . Table. 1 summarizes the analysis conditions.

### 2.2 Experimental Apparatus And Procedure

Fig. 4 shows a sketch of the test loop which was used in this experiment. The test loop consisted of a test section, storage tank, heat exchanger and two pumps. The velocity of flow through the test section was controlled by adjusting the pump rotation speed.

Loop temperature during measurement was maintained by controlling a bypass flow through the heat exchanger. Flow volume was measured with a mass flow meter installed in the test section outlet. The water temperature was monitored by thermocouples installed in the storage tank. The test assembly used in this test was a  $5 \times 5$  square rod array bundle, which consisted of typical cells only. The components of the

test assembly included top nozzle, bottom nozzle, 3 grids and 25 rods.

This experimental apparatus is used to measure the preliminary pressure drop of the newly designed new type grid spacers. In this experiment, the new type grid spacer was set at the middle position among three, and the pressure drop around this was measured by pressure taps which were installed on the walls at several axial levels.

A special method was developed to measure the pressure distribution around the grid spacer. A pressure tap was installed in the rod inserted in to the center of the 5×5 rod array. The diameter of the pressure tap was made small ( $d=0.5\text{mm}$ ) in order to minimize the influence of dynamic pressure. The pressure measurement rod was movable in circumferential and axial directions, so the pressure distribution was measured at different locations over the region from the upstream to the downstream of the middle grid. Table 2 shows the test condition. The tests were performed under steady-state condition.

### 2.3 Verification of Analytical Method by Experiment

The calculated distribution of pressure difference on the flow section inside the grid spacer were compared with the experimental one, to verify this calculation method qualitatively. First, the distribution of pressure difference in the circumferential direction were compared.

Fig.5 shows the location of the pressure difference evaluation points, and Fig.6(A)~(D) shows the comparison between analytical and experimental results in these area. As shown in Fig.2, there were some protrusions in the flow inside the grid spacer; such as springs and dimples to support fuel rods, and they make specific pressure distribution in the circumferential and axial direction of the fuel rod. For example, in Fig.6(C), the pressure difference is smaller in the upstream position on the M/V (right-top and left-bottom position in that figure) than in the downstream position, since the static pressure at this position rises due to the blockage effect of the M/V.

Also, the similar phenomena is observed in the other 2 cross sections, as shown in Fig6(A), (B), due to the blockage effect of the springs and dimples respectively. These figures show that analytical results reproduce these phenomena fairly well.

Second, the distribution of pressure difference in the flow direction were compared between analytical and experimental results. Fig.7 shows the location of the pressure difference evaluation points, and Fig.8 shows the comparison of both results. From Fig.8, it was confirmed that this analysis can simulate the distribution of pressure difference well, even though inside of the grid spacer was complicated by the effects of blockages.

Next, the values of the pressure drop were compared to verify this analytical method quantitatively. For this purpose, 5x5 flow tests and the analysis were performed for several types of grid spacers.

The pressure drop data were obtained from calculations and tests. Table.3 shows the comparison between the experiment and analysis data of the pressure drop. As shown in this table, they show fairly good agreement.

From these results, it was concluded that the adequacy of this analytical method to predict the flow characteristics of the grid spacer was verified.

### 3. Evaluation of Pressure Drop for Full size Grid

As a second step, 3 other types of cell models (thimbleside and corner cell) were also constructed and calculated. The pressure drop of the

full size grid spacer was estimated by combining these results.

### 3.1 Analytical model of a Thimble Cell

The thimble cell is defined as a subchannel that includes one thimble tube in the corner of the cell. There are 4 thimble cells around 1 thimble tube. It is obvious that the pressure drop increases in the thimble cell, because the diameter of the thimble tube is larger than the fuel tube and the flow passage becomes smaller than that of the typical cell. Since the thimble cells neighbour the typical cells, the flow pattern around the thimble cell is closely linked to that of the neighbouring typical cells. So, as shown in Fig. 9, the analysis model for the thimble cell is composed of 4 thimble cells and 1 typical cell, and the cyclic B.Cs are given to the lateral boundaries of the analytical domain, and the calculation for this model has been performed.

The pressure loss coefficient for the thimble cell only has been obtained by extracting typical cell effect from the calculation results, using the parallel channel calculation method. In this calculation, it is assumed that all cells are paralleled and static pressure distribution at inlet/outlet of the cells are uniform.

In this case, the pressure drop of the thimble cell is about 21% larger than that of the typical cell.

### 3.2 Analytical model for Side & Corner Cell

The side cell and the corner cell are parts of the peripheral cell, that form the outer face of the grid spacer. It is obvious that the hydraulic resistance is larger than typical cell at side cells because the outer straps are thicker than the inner one and there are guide vanes and guide tabs at the outer strap, which improve loading performance of the grid spacer.

As to the corner cell, the hydraulic resistance is smaller because of the following reasons; (1) at the corner, there is no guide vane nor guide tab (2) the width of the straps become narrower at the corner. Since side and corner cells are neighbouring the side cells, typical cells and corner cells each other, the flow patterns around these cells were closely linked to that of the surrounding cells. So, as shown in Fig. 10 and 11, the analysis model of the side cell is composed of 2 side cells and 4 typical cells, and the model of the corner cell is composed of 1/4 corner cell and the surrounding 3 typical cells and 2 side cells, and the cyclic B.Cs are given to the lateral boundaries of the analytical domain for both models. The analysis for these models have been performed, and the pressure drop for the side cell only and corner cell only have been calculated from these analytical results. The pressure drop of the side cell and the corner cell are about 35% larger and 47% smaller than that of the typical cell.

### 3.3 Evaluation of Full Size Grid Pressure Drop

By totalling the loss coefficient of each subchannel described in Sec. 2, 3.1 and 3.2, the loss coefficient for the full size grid spacer can be estimated. Table 4 summarizes the calculated results and the number of cells for each type mentioned before. The loss coefficient of the full size grid was obtained by using the parallel channel calculation method. Table 5 shows the comparison between calculated and experimental results, for both the typical cell model and the full size model. In this table, the experimental data for the typical cell was obtained by

the 5×5 cell size test described before, and the loss coefficient of the full size model was obtained by the 17×17 full size test.

The experimental result for the full size grid spacer is larger than that of the 5×5 cell size, and the calculated result simulates this well, moreover the pressure drop value for the full size grid spacer is also estimated successfully.

The procedure developed here is shown in Fig.12. From these results, it is concluded that the pressure drop for the full size grid spacer can be estimated well through these processes.

#### **4. Estimation of the Mixing Characteristics of a Grid using CFD Analysis**

Another subject in PWR thermal hydraulics is to evaluate the DNB (Departure from Nucleate Boiling) performance, and study using the CFD method was carried out as a first step for this purpose.

Up to now, it has been difficult to estimate the DNB performance by CFD calculation, because the DNB phenomena occurs in a 2-phase flow condition, but the CFD can handle single-phase flow only.

It is supposed that the TDC (Thermal Diffusion Coefficient) has influence on the DNB characteristics, and since the TDC value is obtained from the test that performed in single-phase flow, we tried to clear the relation between the TDC and the flow characteristics obtained by CFD. It is easily to suppose that there would be a certain relationship between the TDC and the flow characteristics, because the TDC represent the mixing characteristics between subchannels. So we tried to find the correlation between the TDC factor and the flow characteristics which were obtained from the CFD calculated results.

By comparing TDC value with flow characteristics between 2 different types of grid spacers, the relationship between the TDC and the flow intensity derived from CFD calculation is recognized.

##### **4.1 TDC data of an actual grid spacer**

The TDC values have been obtained from the mixing tests performed at the DNB tests. Fig.13 shows the rod array of the mixing test. A 5x5 test rod bundle was used for this test, and the heater rods were installed in the grid spacer. The tests were conducted in the range of Reynolds number from  $1 \times 10^5$  to  $5 \times 10^5$ , and half of the dummy fuel rods heated up with 100% power, and the rest rods with 25% power, for the purpose of making a temperature gradient in the flow channel. The TDC value was obtained by adjusting the calculated temperature distribution to the measured one at the downstream side of flow channel.

From the mixing tests, 2 sets of TDC data for different type grid spacers (type-A, -B) have been obtained.

The TDC ratio ( $TDC_{(A)} / TDC_{(B)}$ ) for both grid spacers was about 0.58.

##### **4.2 Analysis of the flow pattern of the CFD calculated results**

Fig.14 shows the change of 3 typical flow patterns and the pressure distributions from the CFD calculation, in the cross section downstream of grid spacer. In section I, the flow pattern is represented by 2 types of cross flow lines, one is the flow line across the passage, and the other is the rotating flow line at the center of the cell. These flow lines locate and pressure distribution are symmetrical in each sub-channel. In section II, the center of the rotating flow shifts forward rod surface gradually, and the pressure distribution in each subchannel

becomes un-symmetrical. The intensity of the transverse cross flow relatively becomes stronger, while the quantity of above shift gets larger in area II. Finally the rotating flow disappears, and only transverse cross flow remains as shown in section III. This flow pattern does not change until reaches to the next grid spacer located downstream. In most part of the flow area, the flow pattern is classified as the one in cross section III, and the following data analysis was done on that flow area.

To analyze the flow characteristics related to the TDC value, 2 factors are considered. One of the factor is the intensity of the cross flow, and the other is the average velocity of the cross flow in the cross section. Since the cross flow promotes the mixing between subchannels, the intensity of cross flow would represents the degree of mixing.

On the other hand, the TDC value indicates heat exchange between neighboring subchannels and so the average velocity of the cross flow that represents the flow volume would be related to the TDC value. It was estimated that both factors would relate to the TDC value, because in most of the flow area, only 1 stream of cross flow remains as shown in cross section III, and the intensity of the cross flow was selected to evaluate the flow characteristics. By surveying the flow characteristics carefully, it is recognized that the maximum velocity of the flow located in the cross flow in each cross section. So, the flow intensity, which is defined as a maximum velocity of the cross flow in each cross section, is used as a intensity of the cross flow.

Fig.15 shows the flow intensity transitions for 2 types of grid spacer (type-A, -B).

#### 4.3 Estimation of the Mixing Characteristics

Fig.16 shows the correlation between  $R_{TDC}$  (the TDC ratio) and  $R_{F.I}$  (the flow intensity ratio) for 2 types of grid spacers. The  $R_{TDC}$  and  $R_{F.I}$  are defined as the ratio between 2 types of grid spacers (type-A, type-B) respectively, as follows;

$$R_{TDC} = \frac{TDC_{(B)}}{TDC_{(A)}} \quad [\text{by experiment}]$$

$$R_{F.I} = \frac{\text{Flow intensity}_{(B)}}{\text{Flow intensity}_{(A)}} \quad [\text{by calculation}]$$

In this figure, it was observed that there is a positive correlation between these 2 factors, i.e., the TDC ratio is proportional to the flow intensity ratio. From these results, it is concluded that the TDC value for the new type grid spacer could be estimated from the TDC value of the reference grid and the flow intensity ratio that will be obtained by analyzing CFD calculation results for both reference and new type grid spacers. The schematic diagram of this process is shown in Fig.17.

This method would be used as a design tool for newly designed grid spacers, especially for M/V design. However, since this method does not evaluate the DNB performance directly, more direct evaluation method using CFD would be continued for the next step.

#### 5. CONCLUSION

To improve design in the flow dynamics field, the CFD method to evaluate 3-D flow characteristics for PWR fuel assembly has been developed. The method was successfully verified by experiments performed with an actual grid spacers. This method has already been brought into practical use for design evaluation of the grid spacer for fuel assembly.

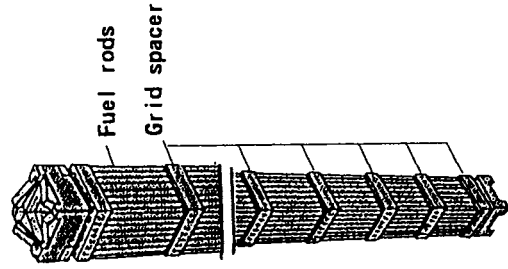


Fig. 2-1 Schematic of PWR fuel assembly

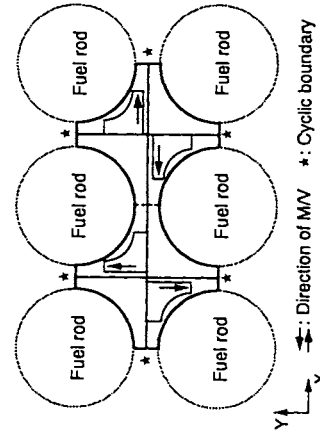


Fig. 3 Analytical Model

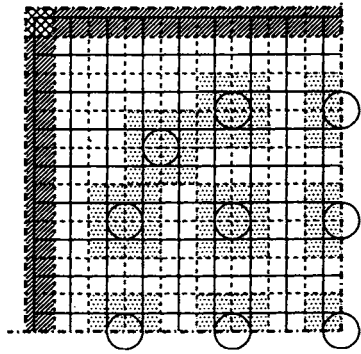


Fig. 1 Types of cells in grid spacer (17x17, 1/4 section)

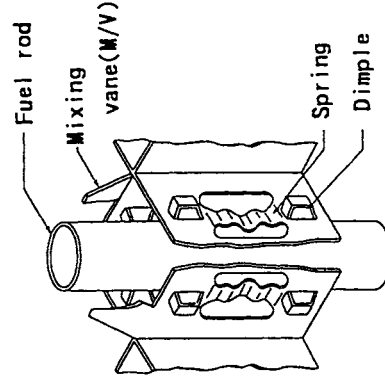


Fig. 2-2 Schematic of Grid spacer

Table 1 Conditions of CFD analysis

Type of grid spacer	14x14 Type	17x17 Type
Reynolds number	$7.7 \times 10^4$	$7.7 \times 10^4$ , $8 \times 10^4$ , $1.5 \times 10^5$
Fluid	Water	Water
Flow velocity in rod bundle	4.2(m/s)	6.0(m/s)
Domain of analysis	2 cells	2 cells
Cell type	Typical	Typical

Table 2 Conditions of flow test

Type of grid spacer	14x14 Type
Test size	5x5 size
Reynolds number	$7.7 \times 10^4$
Fluid	Water
Flow velocity in rod bundle	4.2(m/s)
Fluid temperature	$48 \pm 0.2(^\circ\text{C})$

Table 3 Comparison of pressure drop between test and analysis (for typical cell)

Data	Grid spacer type	
	17x17 Type 1	17x17 Type 2
Normalized Pressure drop †	1.00	1.00
Analysis data ‡	1.05	1.00

† Normalized by test data

Table 4 Summary of analysis for each cell (17x17 type)

Data	Typical cell	Thimble cell	Side cell	Corner cell
Normalized pressure drop data †1	1.00	1.21	1.35	0.53
Percentage of cell numbers ‡2	54.0	34.6	11.7	0.3

†1 Normalized by typical cell pressure drop data

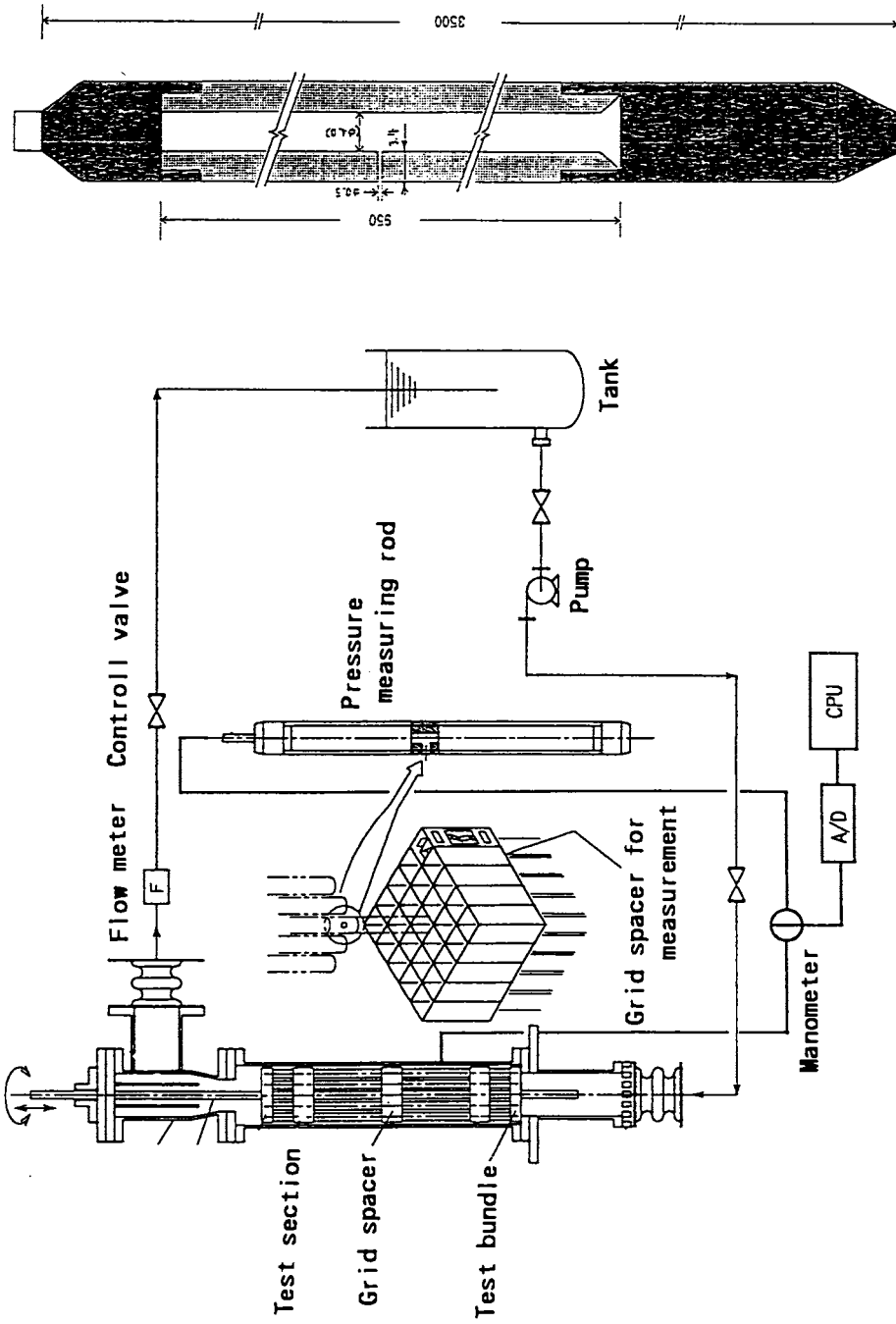
‡2 Percentage of cell numbers for each cell type in full size grid (17x17 type)

Table 5 Comparison of pressure drop between test and analysis (For typical cell and full size grid spacer)

Data	Cell type	Typical cell	Full size
Normalized Pressure drops	Test data	0.88	1.00
	Analysis data	(5x5 cell size)	(full size)
		0.92	1.02

† Normalized by test data for full size grid spacer





Pressure measuring rod

Fig. 4 Schematic of the test loop

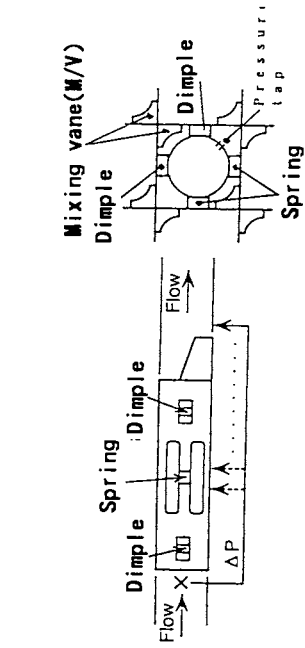


Fig. 7 Locations for the pressure evaluation points (Axial direction)

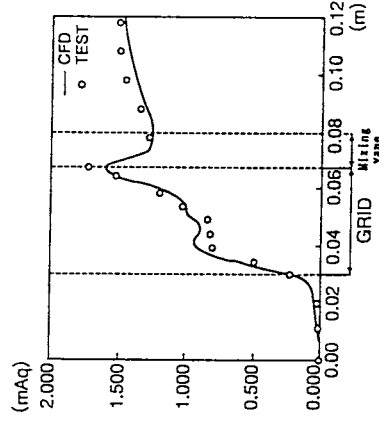


Fig. 8 Comparison between test and analytical results (Axial direction)

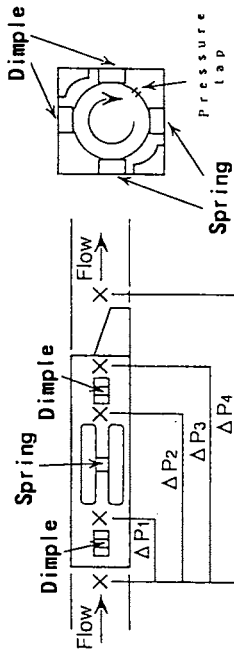


Fig. 5 Locations for the pressure evaluation points (Circumferential direction)

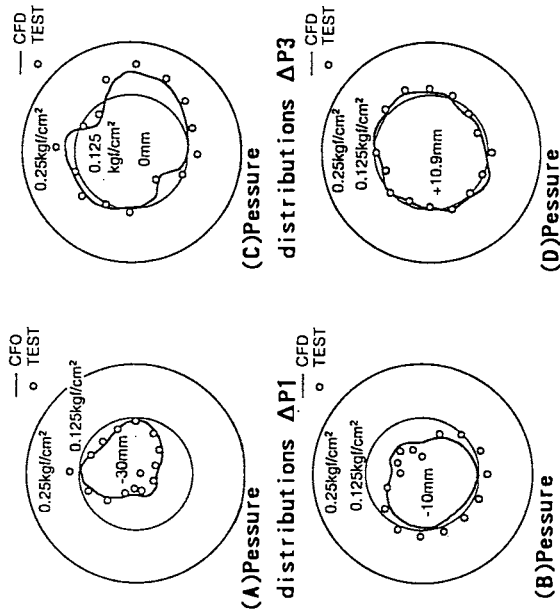


Fig. 6 Comparison between test and analytical results (Circumferential direction)

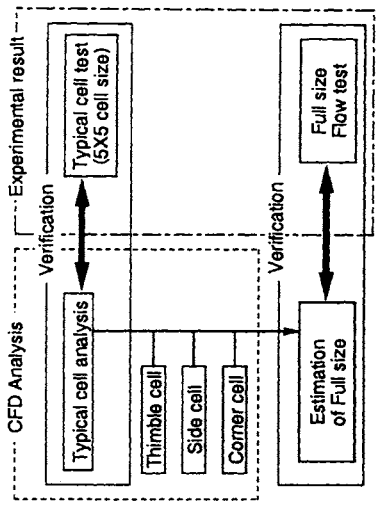


Fig.12 Evaluation method of Full size grid spacer

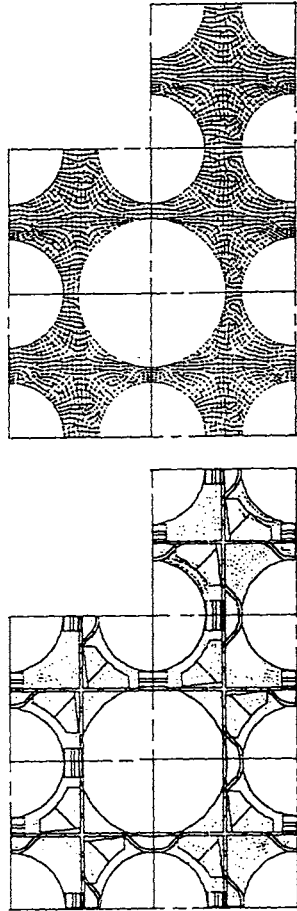


Fig. 9 Thimble cell analysis model

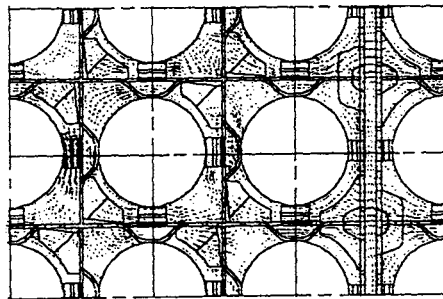


Fig. 10 Side cell analysis model

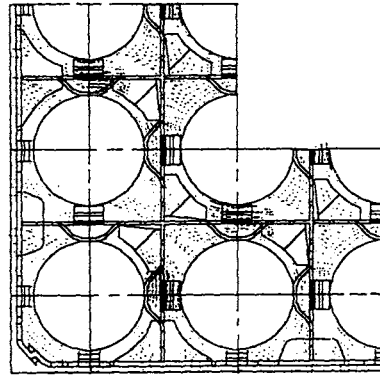


Fig. 11 Outer cell analysis model

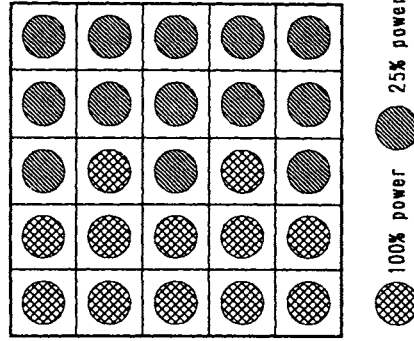


Fig. 13 Rod array of the mixing test

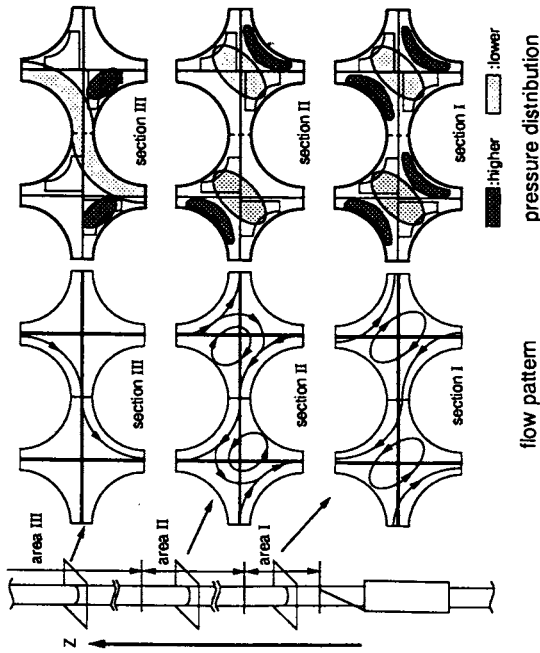


Fig. 14 Transition of flow patterns

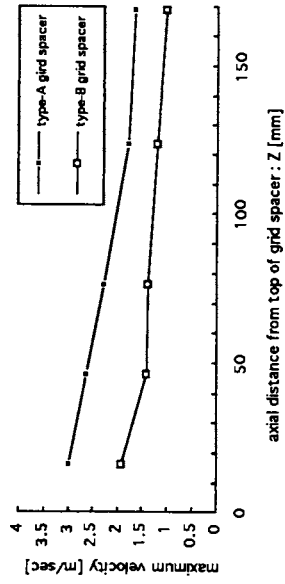


Fig. 15 Axial transition of maximum velocity

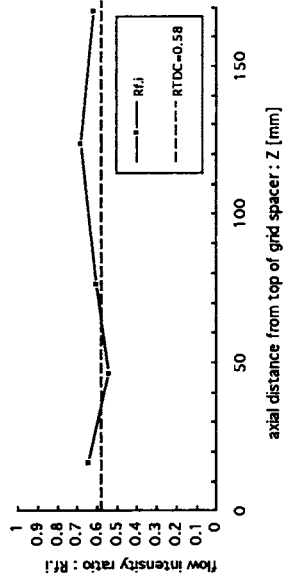


Fig. 16 Comparison between Rf.i and RTDC

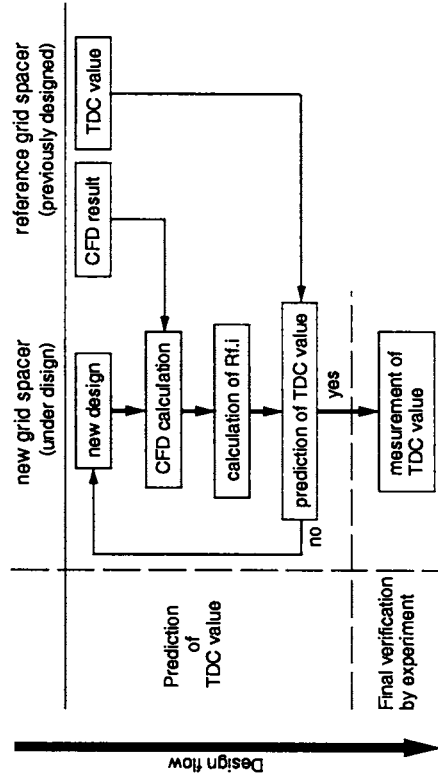


Fig. 17 Design flow of TDC value for new grid spacer